Influence of Number of Turbine Rotations on Numerical Prediction Accuracy of a Three-Bladed NACA0021 VAWT

V. Vishnu Namboodiri and Rahul Goyal

Abstract Performance improvements on wind turbines are emerging due to increased renewable energy demand. The researchers are focusing on improvements in turbine efficiencies. The advancements in numerical simulations immensely support the new design developments and deployment of wind turbines. However, the fidelity and shortcomings of various numerical models are highly challenging to predict accurate results. One of the challenges in numerical simulations is the stopping criteria for the simulations after specific turbine rotations for highly accurate predictions. This paper investigates the influence of turbine rotations on the numerical prediction accuracy for a standalone three-bladed NACA0021 vertical axis wind turbine. The SST k-ω turbulence model is used in 2D turbine configurations. A comprehensive turbine revolution study is carried out for an extensive range of tip speed ratio (TSR) values. The simulation result shows that the operating TSR highly influences prediction accuracy. For lower TSR, a minimal number of turbine rotations are required as compared to higher TSR.

Keywords Vertical axis wind turbine · Numerical simulations · Shear stress transport k-ω · Turbine rotations · Coefficient of power

Nomenclature

D	Diameter of the rotor [mm]
C_P	Coefficient of power [–]
C_T	Coefficient of torque [–]
c	Chord length [mm]
ρ	Density of air [kg/m^3]
N	Number of blades [–]

V. Vishnu Namboodiri · R. Goyal (✉)
Department of Energy Science and Engineering, IIT Delhi, New Delhi 110016, India
e-mail: rahulgoyal@dese.iitd.ac.in

K. M. Singh et al. (eds.), *Fluid Mechanics and Fluid Power, Volume 7*, Lecture Notes in Mechanical Engineering, https://doi.org/10.1007/978-981-99-7047-6_13

V Freestream wind velocity [m/s]
A Swept area [m^2]

1 Introduction

The performance enhancement of wind turbines is of greater interest to the researchers. Over the years, the implementation of medium and small-scale vertical axis wind turbines (VAWTs) has become more challenging as a result of operational instabilities and poor cost-effectiveness. Simultaneously, the wake dynamics and performance in turbulent environments are challenging for horizontal axis wind turbines in larger wind farms. Further, to overcome those shortcomings, various numerical models are proposed by researchers. However, the fidelity of the models is quite reliant on the design problem and the operating environment. The complex design problems are resolved by adopting numerical simulations and subsequent experimentations. Reynolds-averaged Navier–Stokes (RANS) equations are the fundamental basis of numerical methods, and various models are developed based on RANS. However, the prediction accuracies of models are highly influenced by certain numerical, design, and operating parameters. The numerical problems are usually resolved in 2D or 3D domains. However, both environments have their advantages and disadvantages. Many challenges can be identified in the different CFD simulations [1]. One of such challenges is to determine the stopping criteria for the numerical simulations after specific turbine rotations for high accuracy predictions.

2 Literature Review and Objective

The numerical techniques have significantly improved their fidelity. The performances of various models are compared and presented in this section. Chowdhury et al. [2] performed various numerical simulations with multiple turbulence models (i.e., shear stress transport (SST) k- ω, Re-normalization group (RNG) k-ε, and Spalart–Allmaras (SA)) and compared with experimental results in a tilted and upright configuration. The NACA0018 blade profiles were considered for the studies, and the result shows that the SST k-ω turbulence model provides the closest value in comparison with the experimental results. Rogowski et al. [3] also reported similar observations about the superior performance of SST k-ω. One of the prominent advantages of the SST k-ω turbulent model is the improved prediction in the near-wall region, which helps to understand the flow separation behaviors [4]. Rezaeiha et al. [5] performed a comparison of various turbulence models. The models such as the inviscid model, SA, RNG k-ε, realizable k-ε, and SST-based models were considered for 2D numerical simulations. Various turbine configurations, such as NACA 0015 ($N = 1$), NACA 00,118 ($N = 2$), and NACA 0021 ($N = 3$), were

also simulated. SST-based models were observed to predict better than other models. Furthermore, the inviscid model over-predicts for high tip speed ratio (TSR) values. RNG model over-predicts at lower TSR and underpredicts at higher TSR. Rezaeiha et al. [6] performed a study on improving numerical models' accuracy. Their study concludes that the torque value attains convergence after the 20th turbine of rotation. However, this study does not include the variation of numerical prediction accuracy with respect to progress in the TSR values. The literature analysis shows the limited research on the influence of the number of turbine rotations required for convergence for specific ranges of TSR values. This motivated to investigate the effect of a number of turbine rotations on the numerical prediction accuracy in a wide range of TSR.

3 Materials and Methods

This section deals with the methodology for investigating the influence of a number of turbine rotations on torque in a wide range of TSR. The methodology consists of the selection of airfoil, geometry modeling, meshing, numerical settings, analysis, and post-processing. The detailed methodology can be seen in Fig. 1.

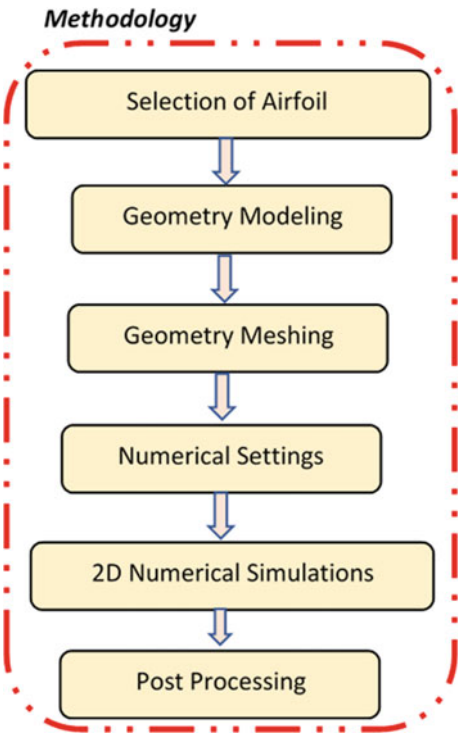

Fig. 1 Methodology

Table 1 Turbine specifications

Parameters	Details/values
Airfoil (–)	NACA0021
Rotor diameter (mm)	1030
Number of blades (–)	3
Chord length (mm)	85.8

3.1 Turbine Specifications

The present study utilizes the NACA0021 as the airfoil profile. The NACA0021 is a thicker symmetric airfoil and can perform well at lower TSR ranges. As the number of blades progresses, the *Cp* value decreases, which is influenced by the airfoil profile. In this context, the number of blades has been fixed as three. The 2D numerical analyses were considered for the present studies due to the availability of validation data from reference literature [7]. Table 1 shows the details of the turbine selected for the present study.

3.2 Geometry Modeling and Meshing

Ansys design modeler has been chosen as the geometrical modeling platform. The turbine specifications are adopted and integrated into a domain to mimic real-life scenarios (see Fig. 2).

Ansys mesh module was considered for the present study. The imported geometry from the design modeler was used for creating an unstructured mesh. Further, the domain is differentiated as inner rotating body, outer rotating body, airfoils, and

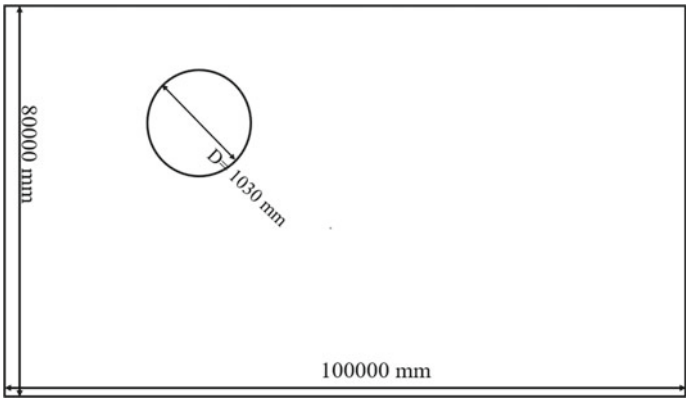

Fig. 2 Fluid domain

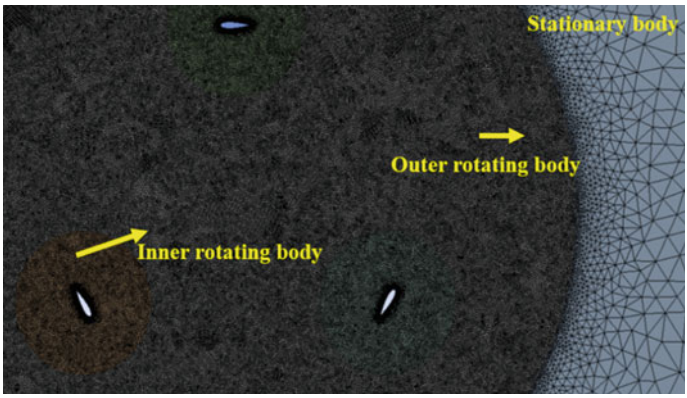

Fig. 3 Domain details

Table 2 Mesh information

Mesh information	Values
No. of elements (–)	15,42,525
Mesh element (–)	All triangle
Inflation layer number (–)	20
Inflation layer growth (–)	1.2
Skewness (–)	$5.64e^{-2}$
Orthogonality (–)	0.9654
Aspect ratio (–)	2.3817
Element size (mm)	Stationary body-115 mm Rotating body-6 mm
Airfoil body (division) (–)	1000

stationary body (see Fig. 3). Table 2 shows the details of the mesh metrics used for the present studies.

3.3 Numerical Settings

The various literatures indicate the reliability of SST-based turbulence models. The present work utilizes SST k-ω for the numerical analysis. The detailed numerical settings adopted for the present study are depicted in Table 3.

Table 3 Numerical settings

Numerical settings	Details
Analysis environment	2D unsteady simulation
Solver	Ansys fluent
Solver type	Pressure based
Fluid	Air
Turbulence model	SST k-ω
Inlet velocity (m/s)	9
Size of the domain (mm^2)	80,000 × 100,000
Inlet boundary condition	Velocity inlet
Outlet boundary condition	Pressure outlet
Blade wall	Moving wall with no-slip boundary condition
Far-field domain	Symmetry
Rotating body	Moving mesh with rotational velocity according to the tip speed ratio
Inlet turbulent viscosity ratio (TVR) (–) and turbulent intensity (TI) (%)	10 and 0.1
Pressure velocity coupling	SIMPLE
Spatial discretization	
Gradient	Least square cell-based
Pressure	Second order
Turbulent kinetic energy	Second order
Specific dissipation rate	Second order
Transient formulation	Second order implicit
Residual	$10^{-3}/10^{-4}$
Degree of rotation (°)	1
TSR range (–)	1.44–3.296
Turbine output parameter (nm)	Average torque (T_{avg})
Number of turbine rotations	25

3.4 Post-processing

The results from 2D CFD simulation are presented for average torque (T_{avg}) and average coefficient of torque (C_T). These variables were calculated using Eqs. (1 and 2) for Cp values with respect to TSR. The torque value was calculated for each rotation with respect to the TSR values for studying the influence of the number of turbine rotations,

$$C_T = \frac{T_{avg}}{T_{available}} = \frac{T_{avg}}{0.5\rho A V^2 R} \tag{1}$$

$$C_P = C_T \times TSR \tag{2}$$

4 Results and Discussion

At TSR 1.67, the evolution of torque values exhibits a steady-state nature after an initial unsteady state.

This shows faster convergence of the torque value and can be observed in Fig. 4. Further, the variation of torque value at TSR 1.67 shows a uniform nature of positive and negative torque generations during the upstream and downstream travel of airfoils. This positive and negative torque combines the overall average torque values at specific TSR and turbine rotations. This trend can be clearly seen in Fig. 5.

The variation of torque value across the turbine rotations is evaluated, and the result shows that at TSR 1.67 no significant change in torque value between the 5th and 25th turbine rotations. This shows the convergence and steadiness of the torque value and is clearly observed in Fig. 6.

At TSR 2.513, as the number of turbine rotations increases, slight changes in the torque value are observed. However, as compared to TSR 1.67, there is a gradual decrease in the torque value. It is observed that after 15th rotation, the torque value starts converging to a steady-state condition with minimal change till 25th rotation of turbine blade and is clearly observed in Fig. 7.

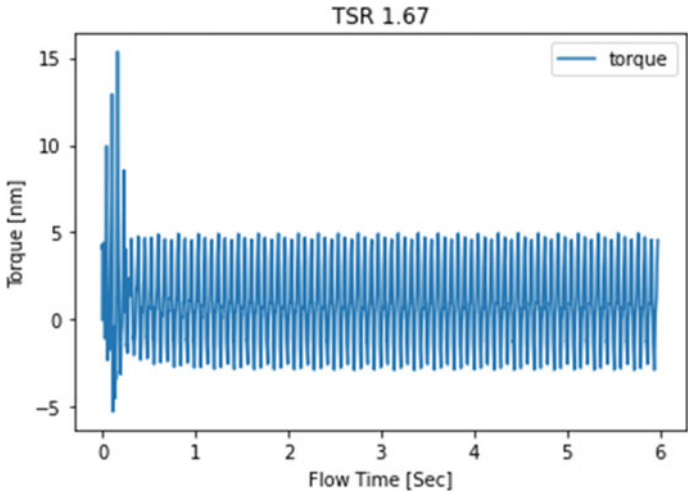

Fig. 4 Evolution of torque

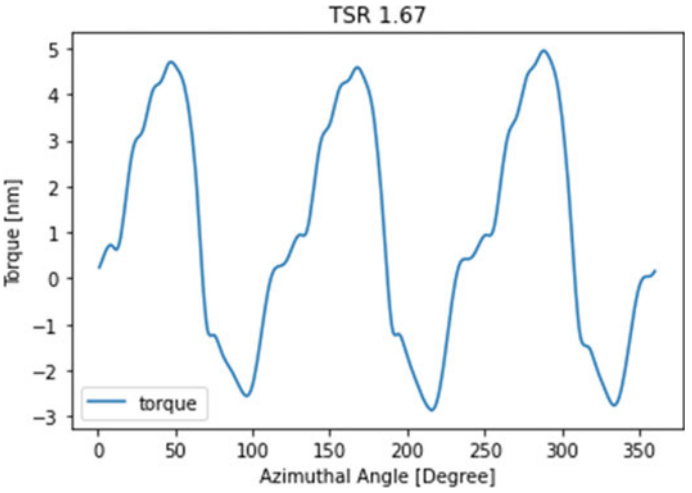

Fig. 5 Torque trend with respect to the azimuthal angle

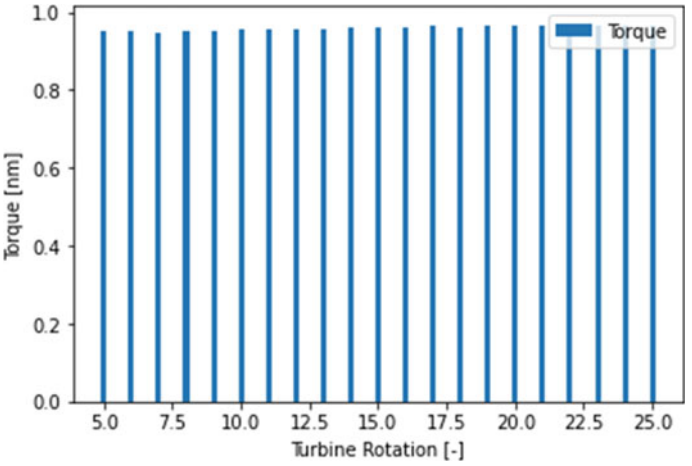

Fig. 6 Variation of torque with number of turbine rotations at TSR 1.67

As the turbine rotations progress at 3.296 TSR, a significant change in torque value is observed between 5 and 10th rotations. This gradual decrease in trend is observed to extend till the 20th rotation. After the 20th rotation, there is no significant variation in the torque value. This infers that the torque value achieved a steady-state value. Thus, numerical simulations for higher TSR turbines require a higher number of turbine rotations to obtain steady-state torque. Figure 8 shows the variation of torque value for turbines operating at higher TSR.

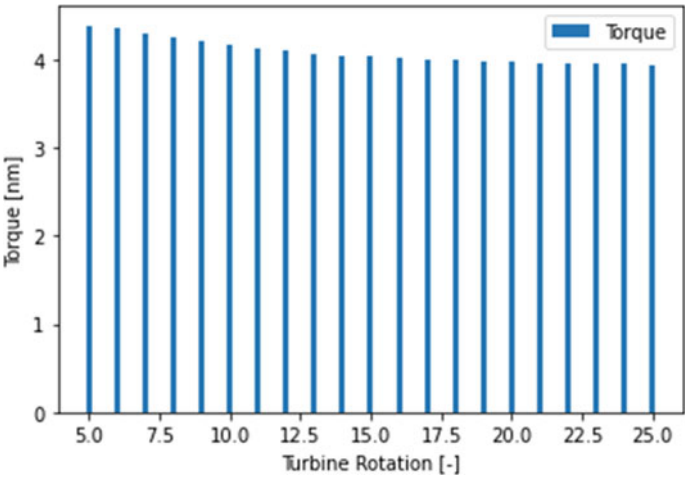

Fig. 7 Variation of torque with the number of turbine rotations at TSR 2.513

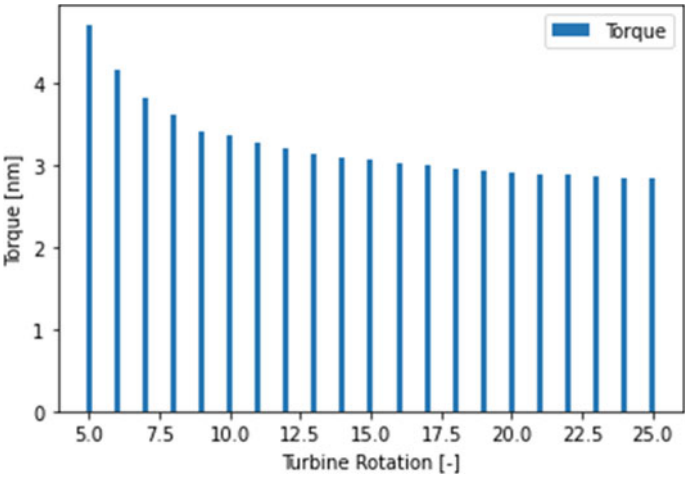

Fig. 8 Variation of torque with the number of turbine rotations at TSR 3.296

The *Cp* at each turbine rotation is computed from torque values for wide ranges of TSR to establish numerical prediction accuracy. Since torque and *Cp* are directly related, the *Cp* values are compared with numerical and experimental results from reference literature [7]. The results infer that at lower TSR, the convergence of the *Cp* value is obtained at a lesser number of turbine rotations. After 2.327 TSR, the influence of the number of turbine rotations is significant and affects results. This trend is observed till 3.296 TSR (see Fig. 9). Further, the analysis revealed that the *Cp* values predicted by the current numerical study outperformed the numerical analysis

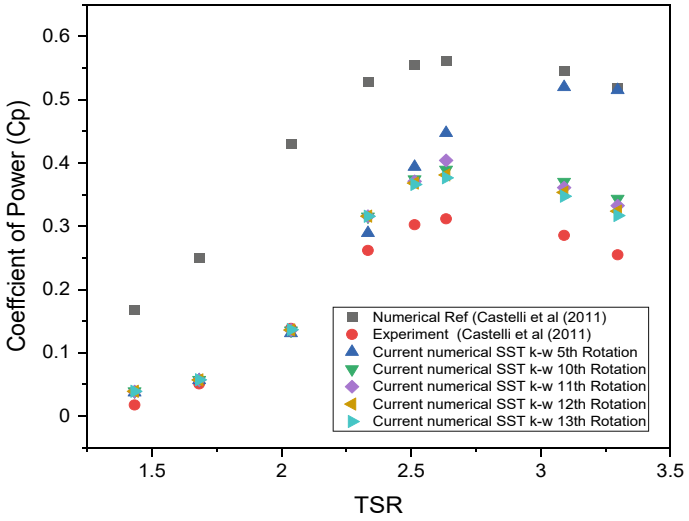

Fig. 9 Variation of C_P with a wide range of TSR

data from the reference literature. Accuracy comparisons with reference literature were carried out and observed that minimal turbine revolutions satisfy the good accuracy at 1.67 TSR. Medium TSR (i.e., 2.513) requires more than ten revolution cycles for good accuracy. Furthermore, higher TSR (i.e., 3.089) requires more than twenty revolution cycles for good accuracy, and similar observations were reported by Rezaeiha et al. [6] (see Fig. 10).

A comparison study with the *Cp* value at the 20th rotation of the turbine is compared with reference literature. The present study agrees well with the experimental reference studies (see Fig. 11).

5 Conclusions

The influence of turbine rotations on numerical prediction accuracy is carried out for a wide range of TSR and compared with the reference literature. The following conclusions can be drawn from the above results.

1. Operating TSR of turbines highly influences the numerical prediction accuracy.
2. At lower TSR, the small number of turbine rotations yield good accuracy. However, at greater TSR, significant changes in the torque value were observed at a low number of turbine rotations.
3. Turbines operating at higher TSR may require more turbine rotations to reach convergence.
4. The number of turbine rotations shall be decided based on the operating TSR range for better numerical prediction accuracy.

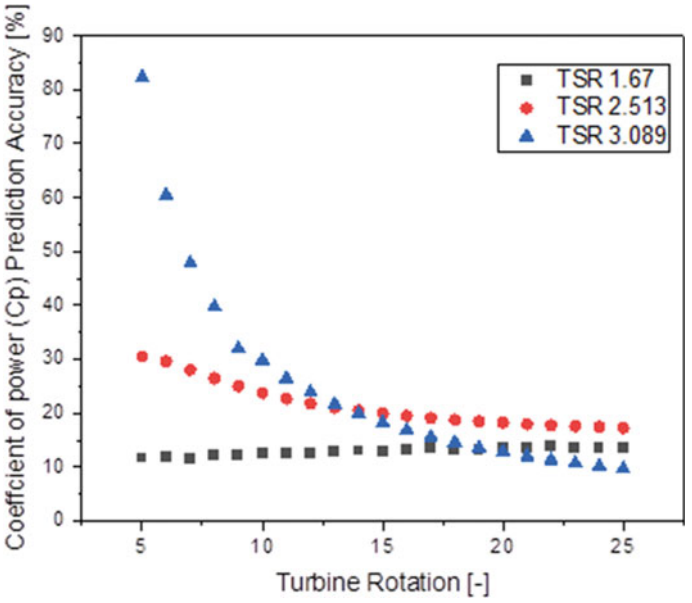

Fig. 10 Variation of accuracy with turbine rotations at various TSR

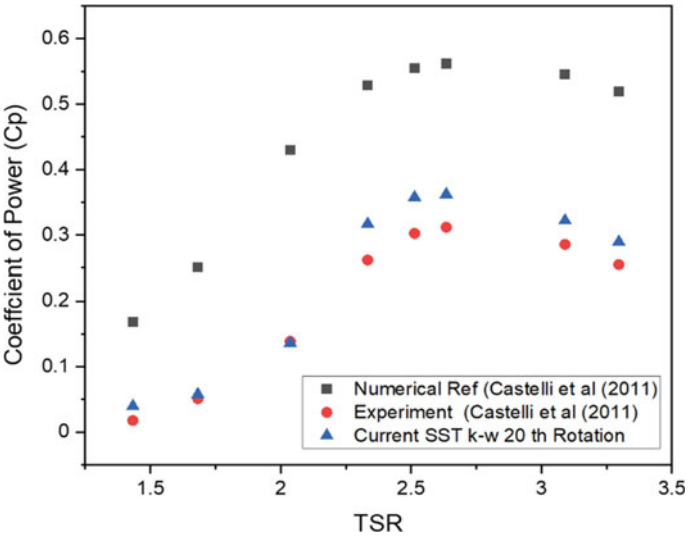

Fig. 11 Performance comparison of reference and current study

Acknowledgements Vishnu Namboodiri V and Rahul Goyal are thankful to the Ministry of Education, India, and the Department of Energy Science and Engineering, Indian Institute of Technology Delhi, for research supports.

References

1. Balduzzi F, Bianchini A, Maleci R, Ferrara G, Ferrari L (2016) Critical issues in the CFD simulation of Darrieus wind turbines. Renew Energy 85:419–435. https://doi.org/10.1016/j.renene.2015.06.048
2. Chowdhury AM, Akimoto H, Hara Y (2016) Comparative CFD analysis of vertical axis wind turbine in upright and tilted configuration. Renew Energy 85:327–337. https://doi.org/10.1016/j.renene.2015.06.037
3. Krzysztof R, Martin Otto Laver H, Ryszard M (2018) Steady and unsteady analysis of NACA 0018 airfoil in vertical-axis wind turbine. J Theoretic App Mech 56(1):203–212. https://doi.org/10.15632/jtam-pl.56.1.203
4. Eltayesh A, Castellani F, Burlando M, Bassily Hanna M, Huzayyin AS, El-Batsh HM, Becchetti M (2021) Experimental and numerical investigation of the effect of blade number on the aerodynamic performance of a small-scale horizontal axis wind turbine. Alex Eng J 60(4):3931–3944. https://doi.org/10.1016/j.aej.2021.02.048
5. Rezaeiha A, Montazeri H, Blocken B (2019) CFD analysis of dynamic stall on vertical axis wind turbines using Scale-Adaptive Simulations (SAS): Comparison against URANS and hybrid RANS/LES. Energy Convers Manage 196:1282–1298. https://doi.org/10.1016/j.enconman.2019.06.081
6. Rezaeiha A, Montazeri H, Blocken B (2019) On the accuracy of turbulence models for CFD simulations of vertical axis wind turbines. Energy 180(838):857. https://doi.org/10.1016/j.energy.2019.05.053
7. Raciti Castelli M, Englaro A, Benini E (2011) The Darrieus wind turbine: proposal for a new performance prediction model based on CFD. Energy 36:4919–4934. https://doi.org/10.1016/J.ENERGY.2011.05.036